3

Role of the Plasma Membrane in Endothelial Cell Mechanosensation of Shear Stress

Peter J. Butler and Shu Chien

3.1 Introduction

Mechanotransduction, which is the process by which cells convert mechanical stimuli to biochemical signaling cascades, is involved in the homeostasis of numerous tissues (reviewed in [21] and [56]). The mechanotransduction of hemodynamic shear stress by endothelial cells (ECs) has garnered special attention because of its role in regulating vascular health and disease. In particular, there is intense interest in identifying the primary molecular mechanisms of the EC sensing of shear stress because its (or their) discovery may lead to clinical interventions in atherosclerosis and other diseases related to mechanobiology.

In this chapter, we address the hypothesis that the plasma membrane lipid bilayer is one endothelial cell mechanosensor. Here we define ''mechanosensor'' as a cellular structure that responds to mechanical stress and initiates mechanotransduction in response to shear stress without involving chemical second messengers. Mechanotransduction, then, is the process by which cells convert this sensory stimulus into changes in biochemical signaling. We define mechanobiology as the study of the entire process of sensation, transduction, and attendant changes in cell phenotype. Because mechanical linkages from the cell surface to lateral, internal, and basal parts of the cell redistribute forces imposed on the cell surface, many structures could serve as mechanosensors. Furthermore, mechanotransduction can involve direct force effects on molecules, diffusion- or convection-mediated transport of molecular second messengers, and the active transport of signaling molecules by molecular motors. Other chapters in this text will address other candidate mechanosensors (e.g., focal adhesions and their integrins). With respect to the membrane, in the context of these definitions, if shear stress induces a perturbation of the membrane constituents, and this perturbation is necessary for mechanotransduction, then the lipid bilayer is considered a mechanosensor. Similarly, if the shear stress acting on the apical portion of the cell leads to the perturbation of the membrane on the basal portion as a result of mechanical linkage, and this membrane perturbation is necessary for subsequent downstream signaling, then we consider the basal membrane also as a mechanosensor.

We first outline the evidence of a role of the plasma membrane in shear stress sensing. We then address the question of whether forces in the membrane are sufficient to elicit changes in lipid dynamics, and we propose novel tools to address whether stresses in the membrane are sufficient to induce lipid-mediated protein signaling. We conclude with a proposal for a unified theory on the role of the plasma membrane in shear sensing. This theory is offered to stimulate discussions of membrane mechanosensing and to foster new research directions.

3.2 Overview of Mechanotransduction

3.2.1 Endothelial Cell Mechanotransduction and Vascular Physiology

The endothelium regulates vascular health by forming a regulated semi-permeable barrier to blood constituents, secreting vasoactive compounds that control vascular caliber, and modulating EC adhesiveness to white blood cells. EC dysfunction can lead to diseases such as atherosclerosis, stroke, and hypertension. The endothelium is subject to hemodynamic forces (e.g., shear stress, τ) that vary temporally, spatially, and in magnitude, depending on the location in the vasculature, the heart rate, and the metabolic demand of tissues (Figure 3.1). Endothelial responses to temporal gradients [5, 11, 12, 33] and spatial gradients [22, 25, 87, 114] in shear stress play a significant role in determining whether ECs exhibit an atherogenic or atheroprotective phenotype [17, 55, 63, 67, 90, 118]. Atherogenic ECs have a higher permeability to low density lipoproteins, greater adhesivity to circulating monocytes, and faster turnover rates. There is a large body of evidence that low and oscillatory shear stress is an atherogenic stimulus, while high and unidirectional shear stress is atheroprotective (e.g., [57]). In addition, EC mechanotransduction plays a role in stent-induced restenosis [71, 113, 120] as well as the development and successful deployment of artificial vascular grafts [89]. The temporal and spatial gradients in shear stress also are important in the coordination of blood flow in the microvasculature [12, 62, 64, 65, 69, 96, 103] and hence in the maintenance of capillary blood pressure and the delivery of oxygen, nutrients, and immunity-related leukocytes to tissues.

3.2.2 Mechanisms of Mechanotransduction

In order to understand the mechanism of the initiation of shear modulation of EC function, there have been many studies searching for primary shear sensors (Figures 3.1 and 3.2). Investigations on the shear modulation of protein products [18], cellular and cytoskeletal orientation [35, 41, 42], production of vasoactive autacoids [31, 47, 66], intracellular calcium concentration [2, 40], gene expression [9, 16, 23, 81, 105], and glycocalyx composition [3] have led to the identification of many molecules involved in mechanotransduction including integrins [57, 60, 76, 86], G-proteins [32, 49, 50, 57, 68], K^+ channels [58, 93, 93, 94], stretch-activated Ca^{2+} channels

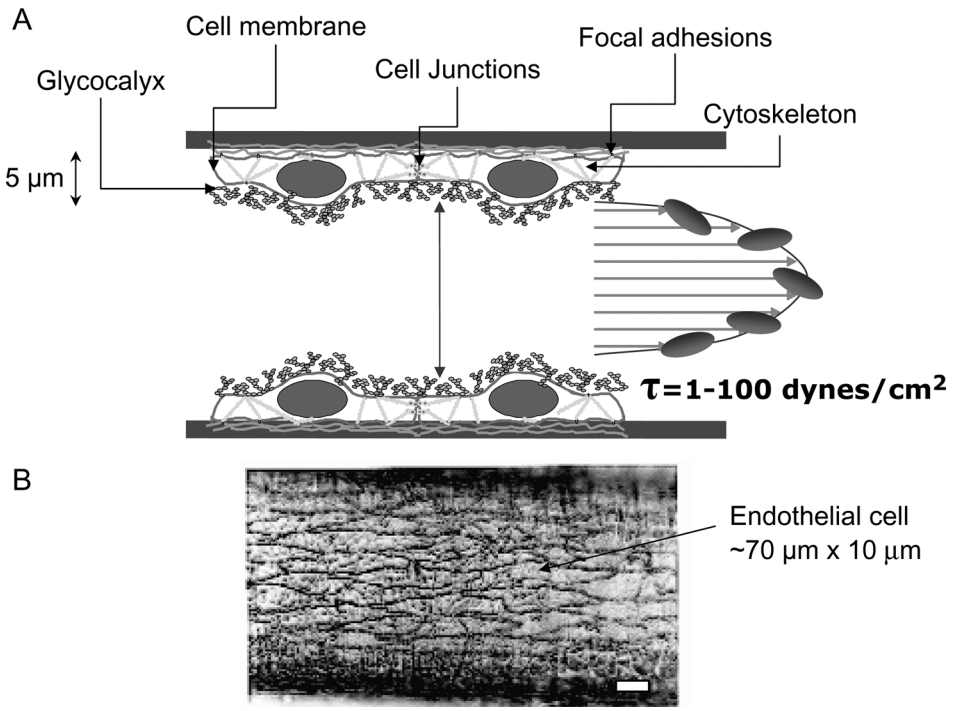

Figure 3.1. Hemodynamics, endothelial cells, and candidate shear sensors. (A) Blood flow induces fluid shear stress on the surfaces of endothelial cells, which distribute the force to multiple structures thought to be involved in mechanotransduction. (B) Silver nitrate staining of endothelial cell borders in isolated arteriole.

[88, 107], surface proteoglycans [6, 83, 106] and cell–cell junctional proteins [83] (reviewed in [21]). Determining whether these molecules are mechanosensors will require sophisticated experimental methods to detect their direct perturbation by shear stress and their role in the conversion of force to downstream biomechanical signaling.

Experimental methods to elucidate EC mechanosensitivity have included engineering analysis, mechanical testing, molecular biological technology, and fluorescence imaging. For example, approaches to elucidate cell mechanics include characterizing the mechanical properties of the EC membrane by micropipette aspiration [100] and atomic force microscopy (AFM) [15, 99], investigating the effects of shear on EC–membrane lipid lateral diffusion [10] and free volume [52], and analyzing the shear-induced deformation of intermediate filaments [54]. Extensive molecular biological investigations have elucidated the signaling pathways that regulate gene transcription in response to shear stress (reviewed in [17]) and have uncovered the genetic endpoints in EC shear sensitivity [16, 36, 81]. Such studies have provided fundamental insights into the force transduction mechanisms and suggest that ECs use multiple cellular structures to integrate the effects of fluid forces into a coordinated cellular response.

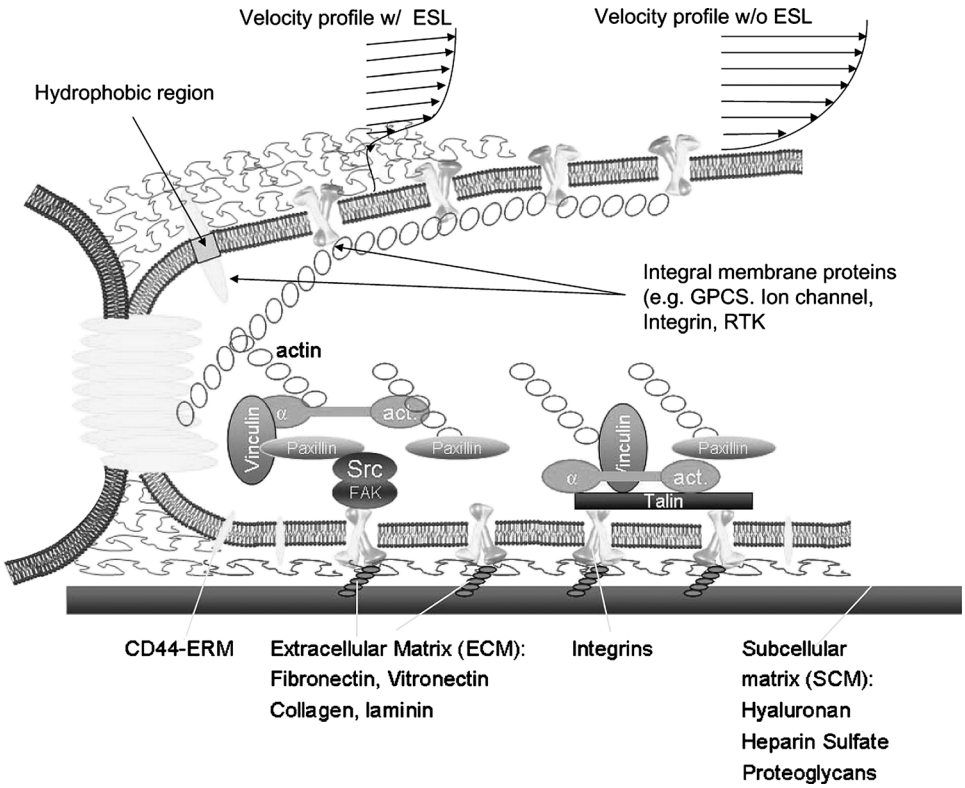

Figure 3.2. Molecular organization in a representative endothelial cell: Membrane, integral membrane proteins, cell junctions, extracellular matrix molecules, and cytoskeleton are represented. Arrows denote velocity near cell membrane. Shear stress (viscosity times velocity gradient) is attenuated in the glycocalyx (endothelial surface layer) compared to areas denuded of the glycocalyx. Stresses may also be transferred to focal adhesions or near focal adhesions where they are amplified.

3.3 The Membrane as a Mechanosensor

3.3.1 Mechanisms of Bilayer Modulation of Protein Function

Circumstantial evidence supports the plausibility that the lipid bilayer is a primary mechanosensor. First, the membrane is exposed to effects of shear stress directly either by its contact with fluid flow, through its interaction with the surface glycocalyx, or by its association with mechanosensitive domains such as focal adhesions (see Figure 3.2). Second, the membrane is a repository for many mechanosensitive proteins [10, 49, 61, 92]. Third, perturbation of EC membrane lipids by shear stress may initiate signaling cascades in ECs leading to altered gene expression [11, 49]. However, the mechanisms of shear perturbation of the membrane or the subsequent molecular mechanisms that link such perturbations with signal transduction have yet to be discovered.

Numerous reviews have been written on the role of the membrane in modulating membrane-associated protein function. For example, Lee [74] discusses the many

biophysical and biomolecular mechanisms by which proteins are modulated by their surrounding lipids. These mechanisms involve the interactions of lipid headgroups with proteins; the effects of differences in hydrophobic thicknesses of proteins and bilayers; the effects of lipid structure on protein aggregation and helix–helix interactions; the role of membrane phases and membrane microviscosity on protein–protein association; the effects on proteins of lipid free volume, bilayer curvature, interfacial curvature, and elastic strain; and the effects on protein inclusions of lateral pressure profile and tension. While the exact mechanism of shear-stress–induced modulation of the interaction of lipids with integral membrane proteins remains to be elucidated, in this chapter we evaluate the two hypotheses of shear modulation of EC membranes for which there exist experimental and theoretical support: shear-induced changes in lipid fluidity and hydrophobic mismatch.

3.3.2 Overview of Membrane Fluidity

Singer and Nicholson [109] first proposed a working model of the cell membrane that allowed for in-plane movement of its components. This model hypothesized that the cell membrane is a thin layer of lipid molecules with protein molecules interspersed throughout. Further studies have revealed that the distribution of lipid molecules is heterogeneous and that some integral membrane protein molecules, being bound to an underlying cytoskeleton, are only intermittently free to move [59]. The term ''lipid fluidity'' has been used to characterize all aspects of lipid mobility, including in-plane and rotational diffusion, and to suggest a mechanism for lipid modulation of protein activity. However, more detailed investigations suggest that lipids modulate protein function through multiple mechanisms [4, 14, 20, 84, 97, 104, 108].

The membrane fluidity of animal cells is determined primarily by the amounts and types of phospholipids, the membrane cholesterol content, and the interaction of lipids with membrane-bound proteins (and the interactions of these proteins with the cytoskeleton). A phospholipid is composed of a hydrophilic head region that is in contact with the extracellular or intracellular space, and two hydrophobic fatty acid chains, which are located in the interior of the membrane and interact with other phospholipid tails. If the tails of the phospholipids are saturated with hydrogen (i.e., with no carbon–carbon double bonds), then they are relatively straight and can pack closely together, leading to a high resistance to lateral movement of membrane constituents and hence a low membrane fluidity. These areas of the membranes tend to be thicker than the more fluid membrane portions. Similarly, increasing the degree of unsaturation, by increasing the number of carbon–carbon double bonds, puts kinks in the otherwise straight chains and makes it more difficult for these types of phospholipids to pack in an orderly fashion. In this case, the membrane is more fluid and thinner. Similarly, cholesterol binds, via a hydrogen bond, to the carboxyl group on the base of the fatty acid and thus intercalates itself into the hydrophilic portion of the membrane [110], thus restricting the movement of lipids and resulting in membrane stiffening.

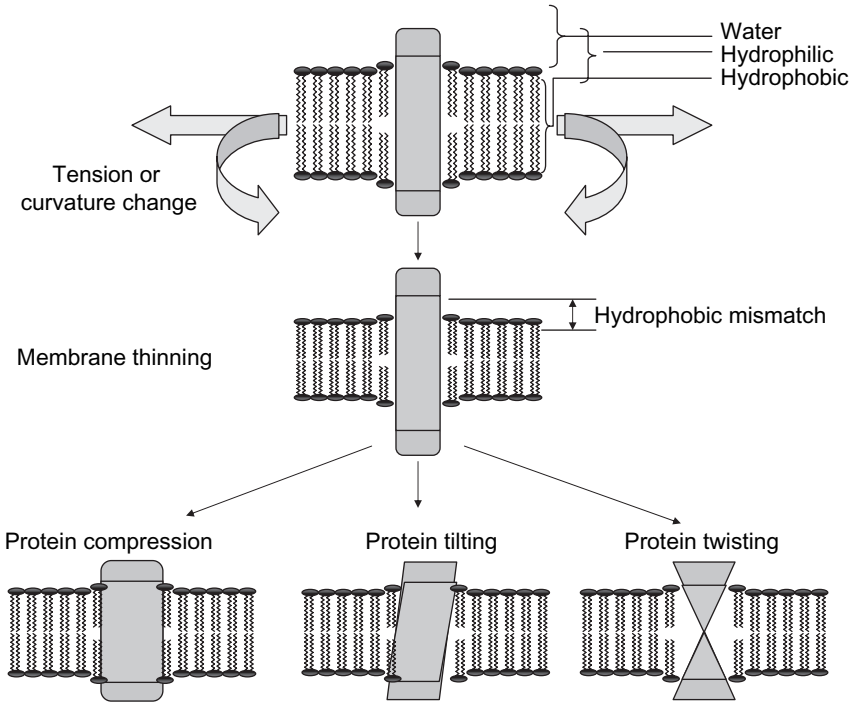

Figure 3.3. Illustration of tension- or curvature-induced changes in hydrophobic thickness of the bilayer: Hydrophobic region of membrane may match hydrophobic thickness of integral membrane proteins. This matching may be perturbed by fluid shear stress leading to membrane tension, which may thin the membrane by direct tension effects or through changes in membrane curvature, leading to alteration of protein conformation by protein compression, tilting, or twisting.

Proteins can also affect membrane fluidity via their interactions with their surrounding lipids [85]. Perturbation of a protein in the lipid medium disturbs the orderly packing of the lipids in an annular region around the protein. Generally, the hydrophilic portion of the lipids (e.g., headgroups) is attracted to the hydrophilic part of the protein. Since the hydrophobic core of the protein may not match the hydrophobic thickness of the lipid bilayer, many proteins protrude out of the membrane, and the lipid environment immediately surrounding the protein is fluidized. Maintaining a separation between fatty acid chains of lipids from opposing leaflets is a high energy process. To minimize the energy required to maintain the membrane integrity around the proteins, often only lipids with longer fatty acid tails will surround the protruding proteins (see Figure 3.3). In this way, proteins determine what types of lipids will surround them. Furthermore, with a high concentration of proteins, these annular regions may overlap, and therefore there is a potential for protein–protein interactions in the annular lipid regions. For proteins that are bound to the cytoskeleton, their presence may lead to an overall stiffening of the membrane.

Each of these properties, that is, fatty acid chain saturation, cholesterol content, and protein content (and protein interaction with the cytoskeleton), are known to be tightly regulated by the cell. When these systems are chronically perturbed, cells can

potentially adjust these properties to maintain an ''optimal'' fluidity. This regulation is known as homeoviscous adaptation [77]. While the notion of a fluidity set-point is still controversial, the homeoviscous adaptation theory has been shown to apply in poikilotherms' adaptation to chronic temperature changes and to cells of hibernating animals. Both poikilotherms and homeotherms adapt to the decreases in cell fluidity induced by cold by synthesizing a greater proportion of unsaturated fatty acids, which, when incorporated into the cells, stabilize membrane fluidity as the temperature falls. If shear stress alters membrane fluidity in a chronic manner, than the cells potentially could adjust their membrane constituents to adapt to this chronic stress. Such adaptation (or lack of) could be a factor, as yet undiscovered, that determines protection from (or propensity for) atherosclerosis.

3.3.3 How Does Lipid Fluidity Affect Proteins?

By restricting (or allowing) movement in the plane of the membrane, changes in lipid fluidity can restrict (or enhance) protein lateral mobility and thus might affect diffusion-dependent protein functions [4]. As an example of diffusion-mediated protein function, G-protein hydrolysis, a process necessary for many agonist-induced changes in the cell, depends on the diffusion of the G-protein from the receptor to a downstream effector. Alterations in this diffusion could potentially affect the equilibrium between receptor/G-protein complexes and effector/G-protein complexes [82]. Since, in equilibrium, fluidity is thought to affect the forward and reverse reaction rates equally [74], it is likely that fluidity changes would affect protein–protein interactions only under nonequilibrium conditions, such as during rapid changes in membrane tension [11].

Finally, lipid fluidity may affect the accessibility of proteins to ligands [104]. According to this concept, tighter packing of lipids causes integral membrane proteins to be pushed out of the membrane and thus make their active sites more available to ligand binding. Increased protrusion of integral proteins out of the membrane could also increase their hydrophobic mismatch and thus alter protein free energy (see next section).

3.3.4 Hydrophobic Mismatch

Because of the energetic cost of exposing hydrophobic amino acid residues to water, it is expected that the hydrophobic region of lipids will match the hydrophobic core of the proteins embedded in the bilayer (Figures 3.2 and 3.3). Equivalently, if the hydrophobic thickness of the membrane changes, then either the lipids will rearrange or the protein will reach a new conformation by tilting, twisting, stretching, or compressing in order to reduce the hydrophobic mismatch (Figure 3.3) [53]. In either case, changes in the membrane thickness will lead to changes in protein conformation. Hydrophbic mismatch can also explain the dimerization of proteins. For example, alterations in lipid fluidity can modulate the protein's local energy environment

by either changing the phase of the lipid immediately surrounding the protein to affect the protein conformation or ameliorating the hydrophobic mismatch. The former effect has been hypothesized to cause the anesthetic effects of haloalthane on nerve function; haloalthane fluidizes the entire membrane and negates the phase change from the protein annular region to the remainder of the lipid bilayer, thus preventing the opening of sodium channels in neurons [115]. If protein dimerization leads to a reduction in protein free energy caused by hydrophobic mismatch, then changes in membrane thickness will lead to dimerization. Similarly, changes in lipid fluidity can affect the hydrophobic mismatch between the lipids and the protein and alter its free energy state [84]. Such changes in free energy may be sufficient to cause a conformational change in a receptor protein, for example, to initiate downstream signaling even in the absence of a ligand.

3.3.5 Role of Membrane Microdomains

Recent studies suggest that mechanically induced stresses are transduced to coordinated biochemical pathways in ECs via the perturbation of the plasma membrane in specialized membrane microdomains, for example, lipid rafts, caveoli [97], focal adhesions [76], and cell junctions [34]. For example, shear-sensitive molecules (G-proteins [92], MAPKs [61], eNOS [37]), reside in $\sim$100-nm–diameter, cholesterol rich, liquid-ordered–phase membrane microdomains termed caveoli and lipid rafts [26, 97]. G_i-proteins (present in lipid rafts [92]) play a role in shear-induced nitric oxide production [93, 111] and in shear-induced MAPK activity [61] in bovine aortic endothelial cells. Focal adhesions and cell–cell junctions may be mechanosensitive membrane domains that may have unique lipid compositions [44, 48, 116]. Recently, Schnitzer [19] has shown that shear stress activates MAPK in caveoli via lipid-mediated mechanisms involving ceramide and sphingomylinase, which may be activated by G-proteins.

Key unanswered questions, however, remain: Is the local stress induced by fluid shear sufficient to perturb molecules in these domains to a sufficient degree to initiate mechanotransduction events, or are the effects of shear stress the results of activation elsewhere and communicated to the membrane via second messengers? Addressing these questions will require increased use of multiscale mechanical models of cells along with optical tools to detect mechanically induced molecular dynamics changes at the submicrometer length scale.

3.3.6 Evidence for Lipid Domains in Cells

There have been excellent studies using electron microscopy to detect caveoli in ECs [97]. However, lipid rafts have been more elusive because they do not have a characteristic stable shape. Thus, indirect means to detect rafts include the observation that certain parts of the membrane float to the top of a density gradient (hence the term ''raft''). Another strategy is to use chain length–sensitive lipoid dyes to take advantage of the fact that lipid rafts and caveoli, because of their increased lipid

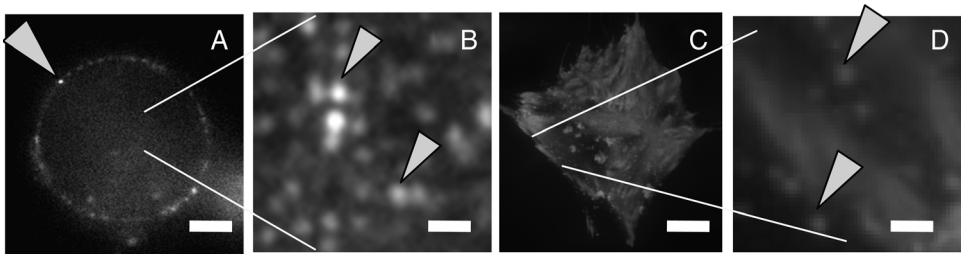

Figure 3.4. Detecting gel-phase lipid microdomains. In order to test whether DiI C_{18} segregates into identifiable gel-phase microdomains, 2-phase vesicles were made from DMPC, DPPC, and DiI C_{18}. At room temperature, dye partitioned into distinct areas presumed to be areas of coalesced gel-phase lipids. Similar structures were identified in BAECs stained with DiI C_{18}. Gel-phase domain formation in GUVs (A, B) and BAECs (C, D). Bars: A = 10 μm, B = 1 μm, C = 10 μm, D = 1 μm.

order, are slightly thicker than bulk plasma membranes. For this chapter, we present the implementation of this strategy in which lipid microdomains are detected using dialkylcarbocyanine, DiI C_{18}, which has the propensity to segregate into the thicker membrane microdomains. First, two-phase vesicles were made from mixtures of imyristoylphosphatidylcholine (DMPC; liquid at room temperature; phase transition temperature 23.5°C) and dipalmitoylphosphatidylcholine (DPPC; gel at room temperature; phase transition temperature 41°C) [70, 80] and DiI C_{18}. Figure 3.4 illustrates how the dye partitiones into distinct areas presumed to be areas of coalesced gel-phase lipids. Similar structures were identified in bovine aortic endothelial cells (BAECs) stained with DiI C_{18}. Similarly, a BAEC culture was stained with both sulfonated (SP-) $DiIC_{18}$ and Alexa-fluor-labeled Cholera-toxin-B (CT-B) (Figure 3.5). CT-B labels GM-1 gangliosides, which are thought to be raft markers [7]. Cells were cultured on borosilicate coverslips and then incubated with a CT-B solution of 25 μg/ml in DPBS on ice for 20 min. The cells were warmed to 37°C and then stained with 10 μM SP-$DiIC_{18}$ using the above procedure. The resulting images were aligned utilizing Autoquant's Autodeblur® software and examined for colocalization of the stains using the NIH ImageJ software. Figure 3.5 (Plate 4) illustrates the colocalization of DiI C_{18} and the raft marker. Thus, it is likely that DiI C_{18}, because of its longer acyl chain length, segregates into lipid domains of comparable thicknesses. Cholesterol is thought to be concentrated in these domains and contributes to its enhanced thickness. We caution that cross-linking of GM-1 with CT-B may induce raft formation. Thus, additional tools are needed to detect rafts in their native state see (see section on fluorescence lifetime later in this chapter).

3.3.7 The Glycocalyx May Modulate the Effects of Shear Stress on Membranes

Recent studies support a possible role of the glycocalyx in modulating mechanotransduction events. Weinbaum et al. [119] and Secomb [102] have shown that the glycocalyx attenuates shear stress near the plasma membrane (see Figure 3.2). Such results suggest that the membrane cannot be a primary sensor of shear stress.

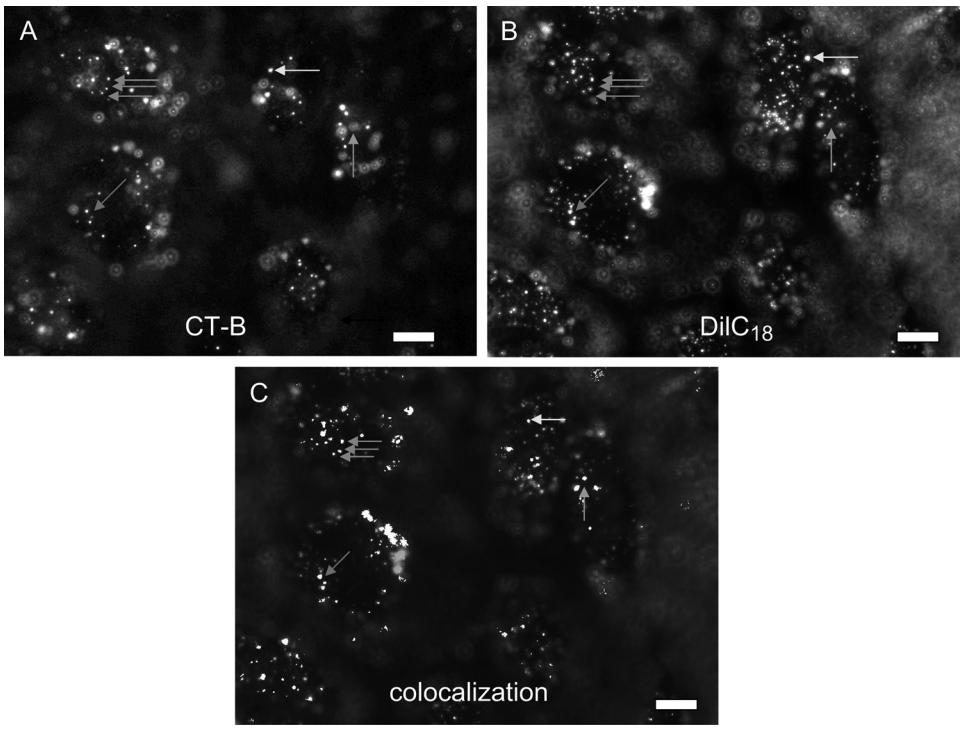

Figure 3.5. Colocalization of long chain lipoid dye and lipid raft markers. BAEC culture was stained with both SP-DiIC$_{18}$ and CT-B. Cells were cultured on borosilicate coverslips, and then incubated with a CT-B solution of 25 μg/ml in DPBS on ice for 20 mins. The cells were warmed to 37°C and then stained with 10 μM SP-DiIC$_{18}$. The resulting images were aligned utilizing Autoquant's Autodeblur® software and examined for colocalization of the stains using NIH's ImageJ software. (A) CT-B staining from channel 1. (B) Sp-DiI C$_{18}$ staining pattern. (C) DiIC$_{18}$ and CT-B colocalization of indicated by white pixels.

Consistent with a role of the glycocalyx in mechanotransduction, Mochizuki et al. [83] showed that degradation of the glycocalyx through hyaluronic acid digestion reduces shear-induced nitric oxide production in isolated arterioles. Similarly, Tarbell and colleagues [30] showed that digestion of heparin sulfate proteoglycans abolishes shear-induced nitric oxide production in cultured ECs. Taken together, these studies support the role of the glycocalyx as a primary mechanosensor of shear stress. It is also possible that the glycocalyx may be necessary for the transmission of fluid forces to the plasma membrane. Consistent with this idea, the glycocalyx has been shown to be anchored to the cell membrane via focal attachment points [112] and through glycoclipid linkages [101]. In addition, the integrated drag on the cell is resisted by focal adhesions near which membrane strain may be greatly amplified [28]. Therefore, it is likely that the glycocalyx can play a role in the transmission of force to the lipid bilayer (i) directly, via attachments to membrane lipids; (ii) indirectly, via integral membrane proteins; and (iii) by modulation of the flow near the lipid bilayer surface.

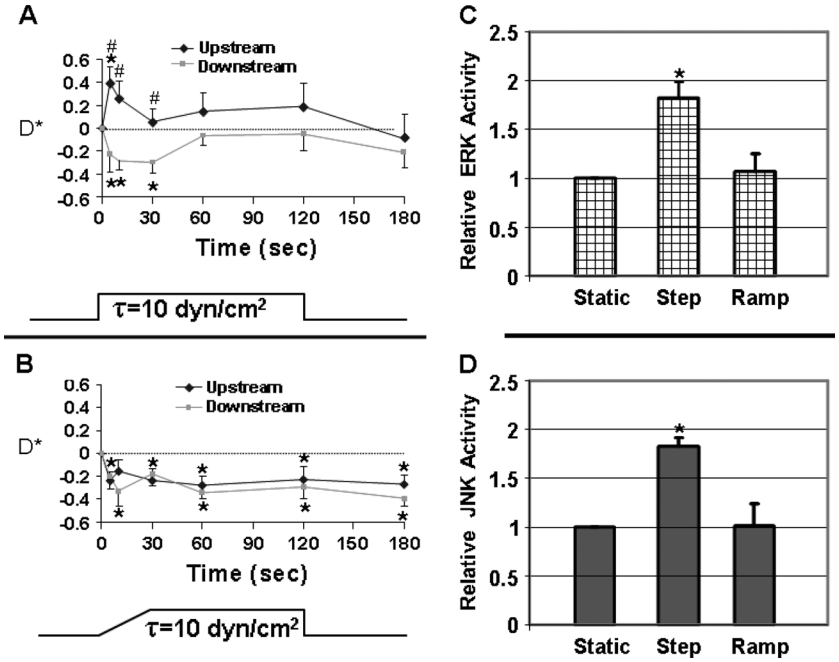

Figure 3.6. Shear stress induces changes in lipid lateral diffusion and activation of MAPK proteins. (A) 10 dynes/cm^2 of shear stress elicit increases and decreases in lipid lateral diffusion on the upstream and downstream sides, respectively, of the EC membrane (D^* = percent change of lipid diffusion from pre-shear values). (B) Shear induced changes in D^* are absent when shear stress is ramped to maximal values. (C) Comparable shear stresses lead to phosphorylation of extracellular-signal regulated kinase (ERK). (D) c-jun N-terminal kinase (JNK). (Adapted from [11] with permission.)

3.3.8 Evidence for Shear Stress Perturbation of Membrane Lipids

Shear stress induces a time- and position-dependent change in lipid lateral diffusion [10] (see Figure 3.6), thus supporting the idea that the cell membrane's proximity to the blood flow makes it a candidate shear-sensitive system. By adapting a confocal laser scanning microscope for measurements of fluorescence recovery after photobleaching (FRAP), Butler et al. [10] made quantitative, two-point, subcellular measurements of membrane fluidity (as quantified by the lipid lateral diffusion coefficient, D) on cells while being subjected to shear stress. Their results have shown that (i) shear stress induces a rapid, spatially heterogeneous, and time-dependent increase in D of a fluorescent lipid probe in the BAEC membrane; (ii) the location, magnitude, and persistence of these shear-induced increases in D depend on the shear magnitude; and (iii) shear stress elicits a secondary (7-min) increase in D. They further demonstrated that the lipid lateral diffusion coefficient (D) of the membrane is sensitive to the temporal gradient in shear stress [11]. A step-τ of 10 dynes/cm^2 elicited a rapid (5-sec) increase of D in the portion of the cell upstream of the nucleus, and a concomitant decrease in the downstream portion (Figure 3.6(A)). A ramp-τ with a rate of 10 dynes/cm^2/min elicited a rapid (5-sec) decrease of D in

both the upstream and downstream portions (Figure 3.6(B)). Thus, it can be concluded that the lipid bilayer can sense the temporal features of the applied τ with spatial discrimination.

Membrane perturbation may activate signaling cascades responsible for changes in gene expression. Butler et al. [11] have shown that a step-shear stress, which increased D, increased the activation of extracellular-signal–regulated kinase (ERK) and c-Jun N-terminal kinase (JNK) (see Figures 3.6(C,D)), which are important signaling molecules for shear stress–related gene expression. Ramp-shear, which failed to increases D, did not result in increases in ERK or JNK. Furthermore, the membrane fluidizer, benzyl alcohol, increased ERK and JNK kinase activity. In contrast, cholesterol, which decreased D, decreased the activities of these MAP kinases, suggesting that stresses in the membrane, as revealed by changes in D, lead to downstream signals that are responsible for altered gene expressions. These results support the hypothesis that the cell membrane plays a role in transducing the magnitude and rate-of-change of shear stress into gene expressions, a feature important in areas of complex flow patterns and abrupt changes in shear stress in the microvasculature during exercise and reperfusion after ischemia.

3.3.9 Other Mechanosensitive EC Functions That Are Modulated by Lipid Membrane Fluidity

Recently, Gojova and Barakat [43] showed that vascular endothelial wound closure under shear stress was modulated by membrane fluidity and dependent on flow-sensitive ion channels. They showed that that reducing EC membrane fluidity in cells near an edge of a wounded monolayer significantly slowed down both cell spreading and migration under flow. Interestingly, when they blocked flow-sensitive K^+ and Cl^- channels, cell spreading was reduced but cell migration was unaffected. Although the relationship between membrane fluidity and ion channel activation in response to flow was not assessed in that study, these findings suggest that membrane fluidity modulates shear-sensitive pathways and the consequent cellular functions such as migration and spreading.

Focal adhesions and integrins are known to be involved in mechanotransduction. Recently, Gaus et al. [38] made measurements of membrane order using two-photon microscopy of the fluorescent membrane probe Laurdan to show that focal adhesions are more ordered than caveolae or domains that stain with cholera toxin subunit B (Ct-B) (presumably lipid rafts) [121]. When cells were detached from the substrate, a rapid, caveolin-independent decrease in membrane order occurred. These results show that phospholipids and cholesterol play important roles in focal adhesion assembly and may have a strong influence on signaling at these sites.

In a related study, Gopalakrishna et al. [44] showed that cholesterol modulates $\alpha_5\beta_1$ integrin functions, suggesting that the lateral mobility of integrin molecules in the plasma membrane, which is influenced by cholesterol content (and membrane fluidity), may regulate the clustering of $\alpha_5\beta_1$ integrin molecules in focal adhesions and, subsequently, their adhesion to the extracellular matrix protein fibronectin and

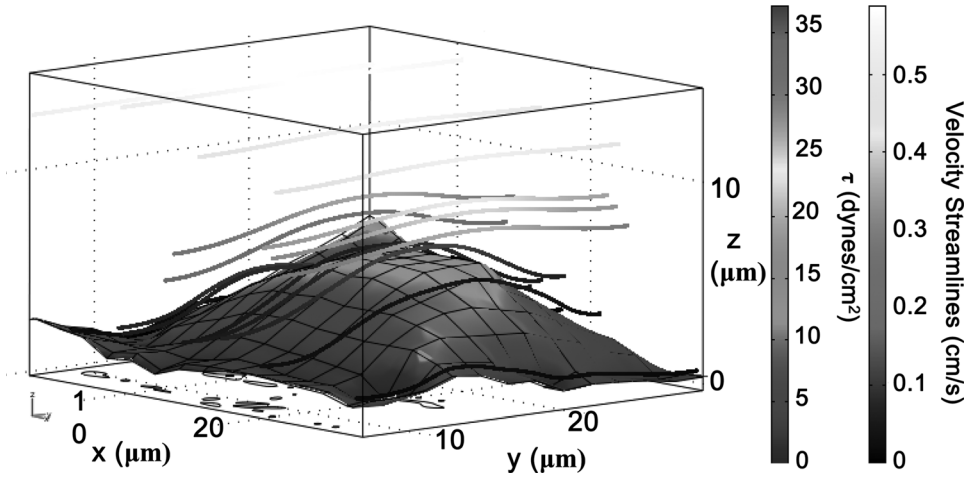

Figure 3.7. Representative subcellular shear stress distribution. A nominal shear stress of 10 dynes/cm^2 was simulated over the solid cell monolayer model in the positive *y*-direction. Model was developed from three-dimensional cellular imaging and quantitative total internal reflection fluorescence imaging of calcein-stained endothelial cells. Finite element analyses of fluid (extracellular) and solid (intracellular) stress distributions were analyzed using computational fluid dynamics and linear elasticity theory. Stress distributions show stress peaks at the apical region over the nucleus while stress is minimum in the valleys between cells. Simulated cell represents a single cell in a monolayer. Simulated velocity field is shown using streamlines. Color plot of shear stress in dynes/cm^2; streamline color corresponds to fluid velocity (cm/s). Axes in m. (Adapted from [27] with permission.)

intracellular protein talin. In that study, the activation of MAPK pathways by the association of fibronectin with $\alpha_5\beta_1$ integrin was suppressed by cholesterol. The role of membrane fluidity in regulating integrin mobility is supported by models of integrin diffusion laterally in the membrane toward focal adhesions [8]. These results also suggest that focal adhesions, like caveoli and rafts, can be thought of as membrane lipid microdomains.

3.3.10 Quantification of Shear-Induced Membrane Stresses

Ferko et al. [29] recently introduced new integrated methods in fluorescence imaging and image processing for the development of solid models with cell-specific topographies and subcellular organelles (Figure 3.7; Plate 5). The goal of this research was to use these methodologies along with quantitative total internal reflection fluorescence microscopy (qTIRFM) to create a cell-specific, multicomponent, three-dimensional solid elastic continuum model of an EC in a confluent monolayer with experimentally determined FAs [28]. Finite element analysis was used to compute stress transmission throughout the EC due to fluid flow applied at the apical surface. This type of cell-specific modeling based on experimentally determined topographies and boundary conditions may help identify potential sites of force-induced potentiation and directional-biasing of cell signaling.

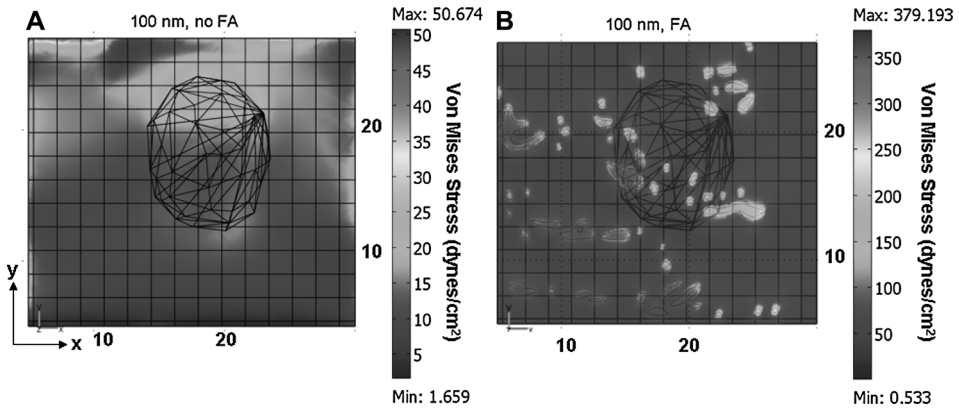

Figure 3.8. Effects of focal adhesion on shear-induced stresses. Von Mises stress distributions were evaluated at $z = 0.1$ μm above the coverslip for (A) model computed without focal adhesions and (B) model solved with focal adhesions. (Adapted from [28] with permission.)

The main contributions of this study were to provide the first quantitative predictions of stress distributions in focally adhered ECs resulting from apically applied fluid flows. These results arose from finite element analysis of a cell-specific model in which surface topography and FA location and area were experimentally determined. The model predicted that shear-induced stresses were generally small but significantly amplified and focused near FAs and the high-modulus nucleus. For example, the inclusion of FAs as attachment locations in a homogeneous linear elastic continuum model resulted in heterogeneous internal stresses, strains, and displacements (see Figure 3.8; Plate 6). Stresses near FAs were nearly 40-fold larger than surface shear stresses, thus supporting the widely held contention that FAs are a means of force amplification of shear stress. The locations and directions of upstream tensile and downstream compressive stresses computed in the vicinity of individual FAs were consistent with the observation of FA growth in the downstream direction of flow and FA retraction in the upstream side, thus providing quantitative information to elucidate the mechanisms of mechanotaxis of ECs [24, 75, 122].

3.3.11 Quantitative Effects of Membrane Tension on Lipid Dynamics and Protein Inclusions

The work of Ferko et al. [28] and Butler et al. [10] support the concept that stresses in the membrane rise to a sufficient degree to induce molecular perturbation. However, the mechanism of shear-induced molecular perturbation of membrane lipids remains unknown. In a theoretical study, Gov [46] provided evidence that changes in the static or dynamic curvatures of the membrane may lead to increased lipid diffusion. To summarize that work, it is postulated that when a flat membrane is curved, the thickness increases, leading to an increased resistance to diffusion. Using molecular diffusion models first proposed by Saffman and Dulbruck [98] in which the diffusion of a cylinder in the plane of the membrane is inversely proportional to the

membrane thickness, membrane thickening would lead to decreases in membrane fluidity and diffusion coefficient. Conversely, when a curved membrane is flattened by a surface tension generated by shear flow, the membrane thins and diffusion increases. Gov's [46] analysis of the effects of shear stress on lipid diffusion fit the data from Butler et al. [10] very well. Interestingly, the changes in the membrane thickness from this analysis can be used to estimate the changes in the hydrophobic matching conditions in a candidate shear-sensitive protein embedded in the lipid bilayer. For a shear stress of 20 dynes/cm^2, Equations 8 and 7 from Gov [46] predict that diffusion will increase by about 40% over pre-shear values, consistent with Butler et al. [10]. Using Equation 4 from Gov, and assuming that the membrane goes from curved to flat during shear application, we can predict that shear stress flattens membrane fluctuations from an initial mean squared curvature of 0.0058 nm^{-2}. This change in curvature would decrease the membrane thickness from 5.0 nm to 3.9 nm (see Equation 4 in Gov [46]), corresponding to a 22% strain in the direction of the bilayer normal (strain parallel to the membrane will depend on the Poisson's ratio of the membrane). This is an appreciable strain and is the same order of magnitude needed to sufficiently alter the free energy of ion channel inclusions in bilayers [1, 45, 91]. Membrane strain in the vicinity of focal adhesions may be even more pronounced, and this would lower the shear threshold for protein activation [39].

3.4 Tools for Measurement of Mechanically Induced Lipid Perturbation

3.4.1 Time-Correlated, Single Photon Counting, and Multimodal Microscopy

Our main hypothesis is that the perturbation of cellular structures by force is accompanied by changes in molecular dynamics. In order to address these fundamental issues in mechanosensing and transduction, Gullapalli, Tabouillot, et al. [51] have developed a hybrid multimodal microscopy-time–correlated single photon counting (TCSPC) spectroscopy system to assess time- and position-dependent, mechanically induced changes in the dynamics of molecules in live cells as determined from fluorescence lifetimes and autocorrelation analysis (fluorescence correlation spectroscopy) (see Figures 3.9 and 3.10). Colocalization of cell structures and mechanically induced changes in molecular dynamics can be analyzed in post-processing by comparing TCSPC data with three-dimensional models generated from total internal reflection fluorescence (TIRF), differential interference contrast (DIC), epifluorescence, and deconvolution [28].

3.4.2 Fluorescence Correlation Spectroscopy

Fluorescence correlation spectroscopy is ideally suited for cellular research because diffusion and chemical kinetics can be measured in very small volumes ($\sim$ 1 fl). A pinhole placed in an image plane of the emission optical pathway defines the confocal observation volume into and out of which fluorescently tagged molecules move (Figure 3.9). The resulting fluorescence fluctuations picked up by the photodetector

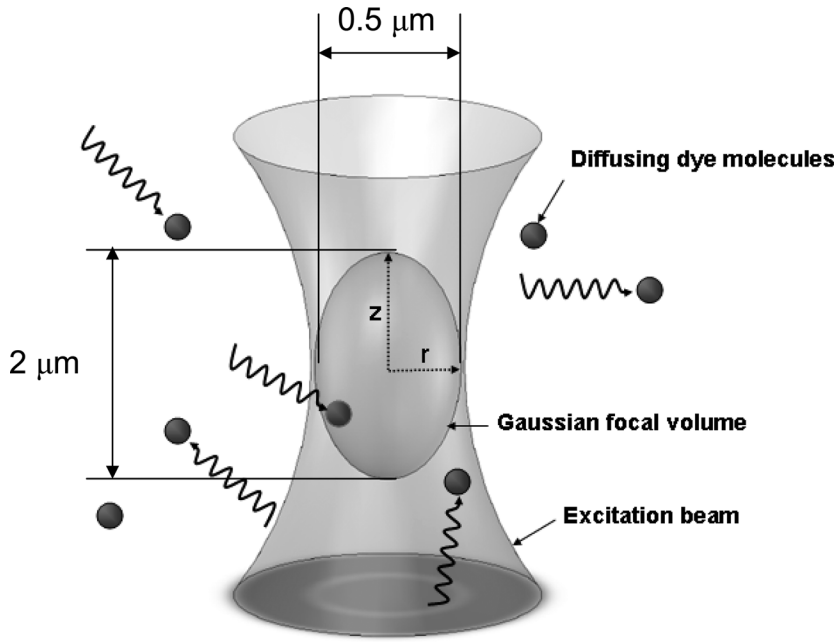

Figure 3.9. Confocal volume for fluorescence correlation spectroscopy. The radial dimension r of the confocal volume is close to the diffraction limit of the objective and is determined by keeping the (r/z) parameter constant (<10) in Equation (3.6) when fitting the autocorrelation curve from R6G molecules in water. The radius thus obtained from experiment is 326 ± 10 nm. Fluorescent molecules are excited by the entire laser beam and fluorescence emission is only collected in the confocal volume. When particles move into and out of the confocal volume in the x, y and z directions, three-dimensional diffusion is considered. When particles only move in the x-y plane, two-dimensional diffusion is considered. (Adapted from [51] with permission)

are translated into current intensity fluctuations. The time autocorrelation curve of this signal can be fit to various formulas to extract physical values for transport phenomena (two- or three-dimensional diffusion, anomalous diffusion, translation) or chemical kinetics [27, 78]. For example, the fluorescence autocorrelation funtion $G(\tau_w)$ can be fit for (two-dimensional) diffusion by

$$G(\tau) = \frac{1}{N} \cdot \left(\frac{1}{1 + \left(\tau_w / \tau_D \right)} \right)$$

where N is the average number of particles, τ_w is the lag time of the autocorrelation function, and τ_D is the characteristic diffusion time, which is related to the diffusion coefficient, D, by $r^2 = 4D\tau_D$.

3.4.3 FCS Measurements of DMPC Giant Unilamellar Vesicles and Endothelial Cell Membranes

In a recent study outlining the use of TCSPC for mechanobiology studies of membranes, Gullapalli et al. [51] performed FCS measurements on DMPC vesicles and EC

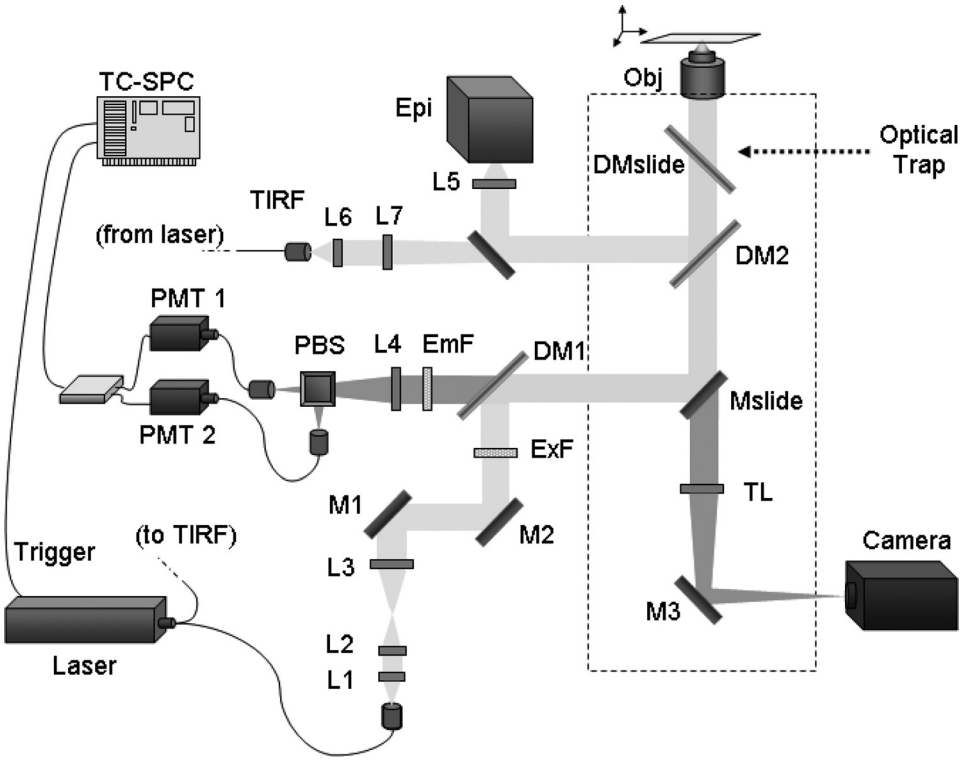

Figure 3.10. Optical setup for TCSPC-multimodal microscopy. The Kr/Ar-ion, diode, or pulsed Nd:YAG laser beam is transmitted via fiber coupling to the TIRF or confocal port. For confocal illumination, upon exiting the fiber, the beam is collimated with lens L1, expanded by L2 and L3, steered by the mirrors M1 and M2, reflected off the dichroic mirror (DM1), and enters the right-side port of the microscope (note that the tube lens for the side port has been removed). After excitation of the sample, the fluorescence emission signal is collimated by the objective and exits the side port, passes through the dichroic mirror, and is focused – using lens L4 – onto the optical fiber, which is connected to the photomultiplier tube (PMT). A polarizing beam splitter (PBS) can be introduced before the fiber to separate light with polarization that is parallel or perpendicular to that of the excitation light. The PMTs convert single photons to electrical pulses, which are routed to the TCSPC board. Laser light from the TIRF system shares the back port of the microscope with the epifluorescence tube (Epi). Lenses L5 and L6 collimate the epifluorescence and TIRF light, respectively. The TIRF illumination is focused at the objective back aperture by lens L7. When the sliding mirror, Mslide1, is removed from the light path, the right-side port is closed and the emission signal can be collected by the camera via the tube lens (TL). In addition, the optical trap can be inserted above the fluorescence cube turret with an infrared dichroic mirror (DMslide) mounted on a custom-built slider (not shown). (Adapted from [51] with permission.)

membranes stained with DiI-C_{18}. Fluorescence of DiI C_{18} was excited with 520-nm light from the CW laser or 532-nm light from the pulsed solid-state laser. Fluorescent light with wavelengths of 545 nm and longer was collected for analysis. The temperature of the media was maintained at 37°C for cells and 26°C for DMPC (phase-transition temperature for DMPC = 24°C). The results were fit using the equation for two-dimensional diffusion. The Results suggest that DiI diffusion in homogenous

model membranes is uniform, but diffusion of the same dye in cell membranes is more restricted (lower diffusion coefficient) and heterogeneous. These data support the hypothesis that these lipoid dyes segregate into membrane micodomains and that time-resolved fluorescence spectroscopy can be used to detect this segregation.

3.4.4 Fluorescence Lifetime

Time-resolved fluorescence lifetime spectroscopy enables the analysis of subtle changes in the photophysics of fluorescent molecules [72]. When a fluorescent molecule is excited to a higher energy state using a picosecond pulse of laser light, it remains in the excited state for a finite time before it decays to the ground level energy state. Using a high-frequency pulsed laser, histograms of photon emission times relative to excitation times can be generated and fit with a negative exponential (or multiple exponentials) with a characteristic decay time (or lifetime), τ_F (different than the characteristic diffusion time, τ_D, of FCS). The Fluorescence lifetime depends on local molecular microenvironmental factors, including ionic strength, hydration, oxygen concentration, binding to macromolecules, and the proximity to other molecules that can deplete the excited state by resonance energy transfer [72]. The fluorescence lifetime and quantum yield are related to the intrinsic photophysical characteristics of a fluorescent molecule such as radiative and nonradiative decay mechanisms. The fluorescence quantum yield, Q, is the ratio of the number of photons emitted to the number of photons absorbed, according to

$$Q = \frac{k_r}{k_r + k_{nr}}$$

where k_r and k_{nr} are the radiative and nonradiative decay rates of the molecule, respectively. Fluorescence lifetime is given by

$$\tau_F = \frac{1}{k_r + k_{nr}}$$

The value for k_{nr} depends on the mode of the nonradiative decay, such as collisional quenching, hydration, and vibrational relaxation. Thus, any alteration of k_{nr} also leads to a detectable change in the value of the fluorescence lifetime.

The value for fluorescence lifetime is obtained by an iterative reconvolution of an instrument response function (IRF), with the fluorescence intensity using an assumed decay law, which can be approximated by a sum of exponentials [72]:

$$I(t) = \sum_i \alpha_i \exp(-t/\tau_{Fi})$$

where α_i is the fraction of molecules with lifetime τ_{Fi}, normalized to unity. Fluorescence lifetimes are independent of fluorescence probe concentrations and can provide information not obtainable from intensity variations alone. When polarized light is used to excite a molecule whose excitation dipole is oriented parallel to the polarization of the pulse, it is possible to separate the parallel and perpendicular components of the emitted fluorescence signal and to extract rotational diffusion constants [72].

As an example of how fluorescence lifetime can probe membrane microdomains, BAECs were labeled with either $DiIC_{12}$ or $DiIC_{18}$ and fluorescence lifetime (FL) measurements were taken on the cell membrane (Figure 3.11). Histograms suggest that the FL of $DiIC_{18}$ is twofold greater than the FL of $DiIC_{12}$, suggesting that nonradiative energy transfer (dictated by k_{nr}) is greater for the short-chain–length dyes. Since the fluorophore of these two probes is identical, these differences in τ_F indicate that $DiIC_{18}$ is probing a more restrictive environment than $DiIC_{12}$. The absolute value of the $DiIC_{18}$ τ_F is consistent with its probing of gel-phase lipid domains (Figure 3.12) [95]. Further evidence of the association of $DiIC_{18}$ with membrane domains is shown in Figure 3.5 (Plate 5), where DiI C_{18} staining was found to colocalize with FITC- labeled cholera toxin, a raft marker.

3.5 A Proposed Model of Lipid-Mediated Mechanotransduction of Shear Stress

We conclude this chapter by proposing a model for membrane mechanosensing and mechanotransduction. Elements of this model are supported by experimental observations and theoretical predictions. We propose that the membrane is naturally curved or undergoing curvature fluctuations and is flattened when subjected to tension by the integrated effects of fluid shear stress. This effect may be felt on the apical surface of the cell, where the glycocalyx transmits drag to the membrane directly, or where the shear stress impacts on the membrane directly in glycocalyx-deficient cells. Similarly, membrane perturbation by shear stress may occur on the basal membrane near focal adhesions, where membrane stresses are amplified. Flattening of the membrane has three effects that occur simultaneously. First, thinning due to reduction in curvature induces an increased lateral diffusion of lipids and membrane-bound proteins that may influence their interactions with downstream effectors. Second, thinning induces an enhanced hydrophobic mismatch that imposes an energy penalty on transmembrane proteins. These proteins change their conformations to reduce this energy penalty, thus altering their function. The confrontation change may lead to ion channel flux, G-protein–coupled receptor activation [79], or other changes. Third, membrane bending changes the lateral pressure profile in the membrane and increases the pressure in one leaflet while reducing it in the other [13]. This pressure profile can lead directly to changes in protein function and in the distribution of the (more mobile) cholesterol. Cholesterol translocation from one leaflet to another may also function to dissipate the stress in the membranes [73], which might explain the transient nature of shear-induced changes in lipid lateral diffusion [11].

Some elements of this model can be tested experimentally with optical methods based on time-correlated single photon counting. For example, shear-induced changes in lipid diffusion can be assessed with FRAP and FCS, while changes in the interaction with the membrane-domain–selective dyes such as DiI can be elucidated with fluorescence lifetime imaging microscopy (FLIM). More sophisticated experiments in which proteins are engineered with conformation-sensitive fluorescence moieties can be used to detect lipid-mediated conformational changes in

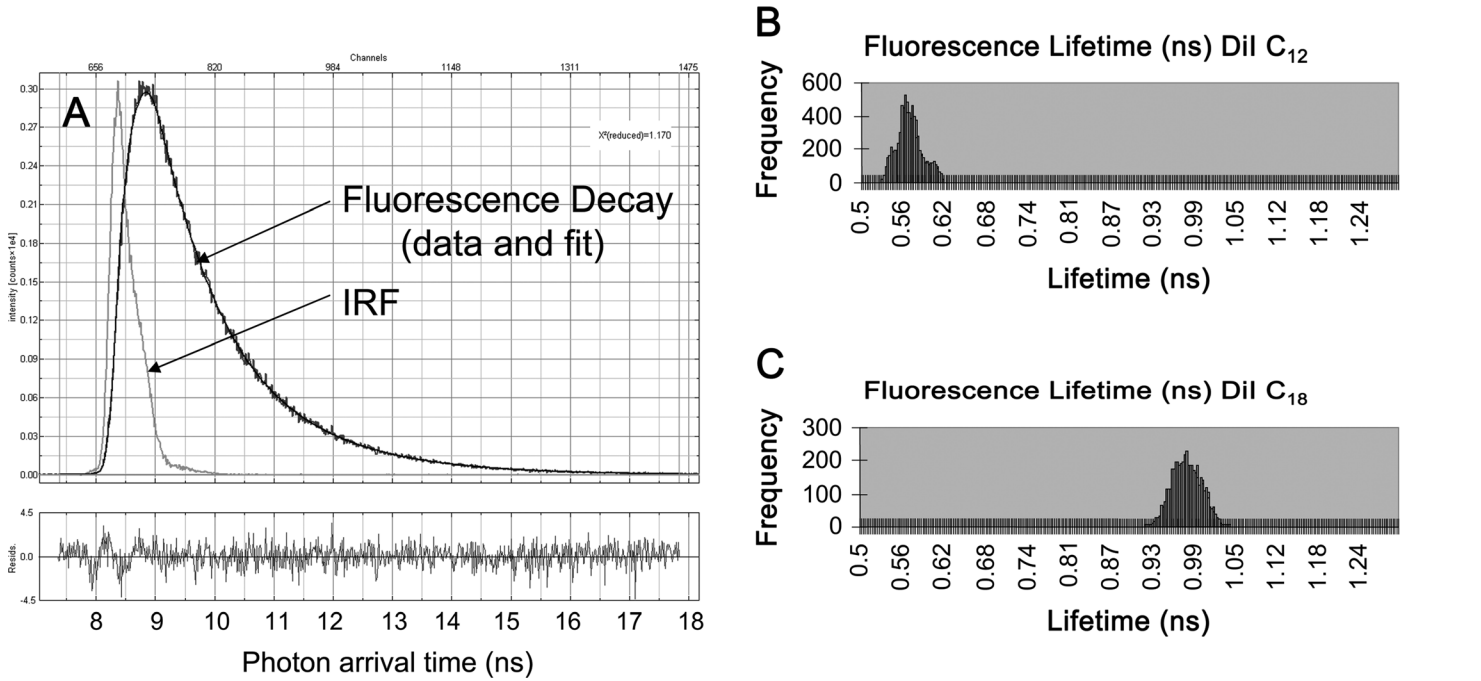

Figure 3.11. Fluorescence lifetime analysis of lipoid dyes. (A) Fluorescence decay (blue line) and instrument response function (red line) for DiD fluorescence in ethanol. The decay histogram is fit with a double exponential (black line) to obtain the fluorescence lifetime. The x^2 value of the fit is 1.17. The full width at half maximum (FWHM) of the instrument response function is $\sim$ 300 ps. (B, C) Fluorescence lifetime of (B) DiI C_{12} and (C) DiI C_{18} in bovine aortic endothelial cells.

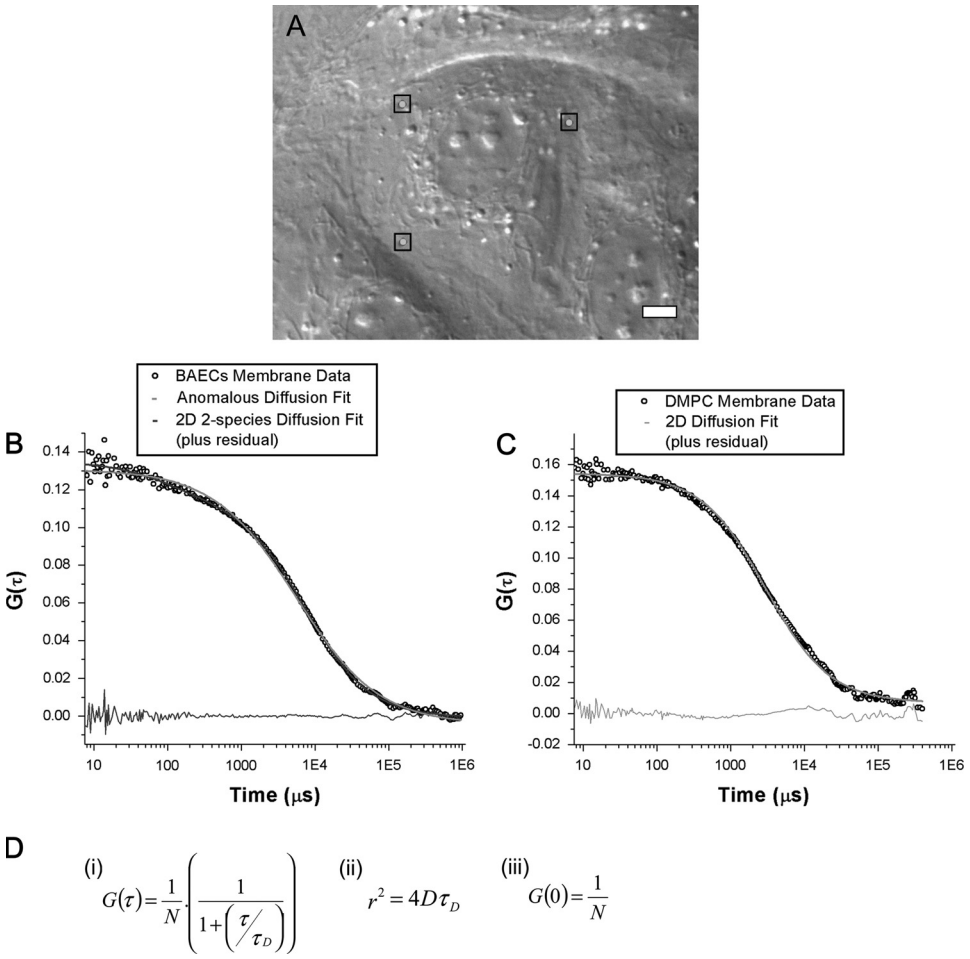

Figure 3.12. Use of fluorescence correlation spectroscopy for membrane mechanobiology. (A) Differential interference contrast images of endothelial cells. (B) Representative autocorrelation curves of fluorescence obtained from model membranes and DiI C_{18}. (C) Representative autocorrelation curves of fluorescence obtained from intact cellular membranes and DiI C18. (D) Equations: (i) equation is fit to autocorrelation curve by adjusting diffusion time, (ii) equation or two-dimensional diffusion to obtain diffusion coefficient from characteristic diffusion time, (iii) y-intercept of autocorrelation gives absolute molecular concentration (N, number of molecules) in confocal volume.

integral membrane proteins. Other techniques such as fluorescence resonance energy transfer [117] based on spectral, intensity, or fluorescence lifetime changes may reveal time- and membrane-dependent alterations of protein conformation in response to fluid shear stress. While these fluorescence techniques require extensive control experiments in order to interpret molecular-level changes, the accessibility of these techniques makes them the method of choice for single-molecule mechanobiology experiments [51]. In addition, these experimental observations, coupled with more refined mechanical models based on cellular ultrastructure, will help elucidate the fundamental underpinnings of mechanotransduction.

REFERENCES

[1] Andersen, O. S., et al. Ion channels as tools to monitor lipid bilayer-membrane protein interactions: Gramicidin channels as molecular force transducers. *Methods Enzymol*. **294**, 208–224 (1999).
[2] Ando, J., Ohtsuka, A., Korenaga, R., Kawamura, T., & Kamiya, A. Wall shear stress rather than shear rate regulates cytoplasmic Ca^{++} responses to flow in vascular endothelial cells. *Biochem. Biophys. Res. Commun*. **190**, 716–723 (1993).
[3] Arisaka, T., et al. Effects of shear stress on glycosaminoglycan synthesis in vascular endothelial cells. *Ann. N.Y. Acad. Sci*. **748**, 543–554 (1995).
[4] Axelrod, D. Lateral motion of membrane proteins and biological function. *J. Membr. Biol*. **75**, 1–10 (1983).
[5] Bao, X., Clark, C.B., & Frangos, J. A. Temporal gradient in shear-induced signaling pathway: Involvement of MAP kinase, c-fos, and connexin43. *Am. J. Physiol Heart Circ. Physiol* **278**, H1598–H1605 (2000).
[6] Bevan, J. A. & Siegel, G. Blood vessel wall matrix flow sensor: Evidence and speculation. *Blood Vessels* **28**, 552–556 (1991).
[7] Boesze-Battaglia, K. Isolation of membrane rafts and signaling complexes. *Methods Mol. Biol*. **332**, 169–179 (2006).
[8] Broday, D. M. Diffusion of clusters of transmembrane proteins as a model of focal adhesion remodeling. *Bull. Math. Biol*. **62**, 891–924 (2000).
[9] Brooks, A. R., Lelkes, P. I., & Rubanyi, G. M. Gene expression profiling of human aortic endothelial cells exposed to disturbed flow and steady laminar flow. *Physiological Genomics* **9**, 27–41 (2002).
[10] Butler, P. J., Norwich, G., Weinbaum, S., & Chien, S. Shear stress induces a time- and position-dependent increase in endothelial cell membrane fluidity. *Am. J. Physiol Cell Physiol* **280**, C962–C969 (2001).
[11] Butler, P. J., Tsou, T. C., Li, J. Y., Usami, S., & Chien, S. Rate sensitivity of shear-induced changes in the lateral diffusion of endothelial cell membrane lipids: A role for membrane perturbation in shear-induced MAPK activation 1. *FASEB J*. **16**, 216–218 (2002).
[12] Butler, P. J., Weinbaum, S., Chien, S., & Lemons, D. E. Endothelium-dependent, shear-induced vasodilation is rate-sensitive. *Microcirculation* **7**, 53–65 (2000).
[13] Cantor, R. S. Lipid composition and the lateral pressure profile in bilayers. *Biophys. J*. **76**, 2625–2639 (1999).
[14] Casey, P. J. Protein lipidation in cell signaling. *Science* **268**, 221–225 (1995).
[15] Charras, G. T. & Horton, M.A. Determination of cellular strains by combined atomic force microscopy and finite element modeling. *Biophysical Journal* **83**, 858–879 (2002).
[16] Chen, B. P., et al. DNA microarray analysis of gene expression in endothelial cells in response to 24-h shear stress. *Physiol Genomics* **7**, 55–63 (2001).
[17] Chien, S. Molecular basis of rheological modulation of endothelial functions: importance of stress direction. *Biorheology* **43**, 95–116 (2006).
[18] Chien, S., Li, S., & Shyy, Y. J. Effects of mechanical forces on signal transduction and gene expression in endothelial cells. *Hypertension* **31**, 162–169 (1998).
[19] Czarny, M. & Schnitzer, J.E. Neutral sphingomyelinase inhibitor scyphostatin prevents and ceramide mimics mechanotransduction in vascular endothelium. *Am. J. Physiol Heart Circ. Physiol* **287**, H1344–H1352 (2004).
[20] Dan, N. & Safran, S. A. Effect of lipid characteristics on the structure of transmembrane proteins. *Biophys. J*. **75**, 1410–1414 (1998).
[21] Davies, P. F. Flow-mediated endothelial mechanotransduction. *Physiological Reviews* **75**, 519–560 (1995).

[22] Davies, P. F., et al. Spatial relationships in early signaling events of flow-mediated endothelial mechanotransduction. [Review] [48 refs]. *Annual Review of Physiology* **59**, 527–549 (1997).
[23] Davies, P. F., Polacek, D. C., Handen, J. S., Helmke, B. P., & DePaola, N. A spatial approach to transcriptional profiling: Mechanotransduction and the focal origin of atherosclerosis. *Trends in Biotechnology* **17**, 347–351 (1999).
[24] Davies, P. F., Robotewskyj, A., & Griem, M. L. Quantitative studies of endothelial cell adhesion. Directional remodeling of focal adhesion sites in response to flow forces. *J. Clin. Invest*. **93**, 2031–2038 (1994).
[25] DePaola, N., Gimbrone, M. A., Jr., Davies, P. F., & Dewey, C. F., Jr. Vascular endothelium responds to fluid shear stress gradients. *Arterioscler. Thromb*. **12**, 1254–1257 (1992).
[26] Dietrich, C., Yang, B., Fujiwara, T., Kusumi, A., & Jacobson, K. Relationship of lipid rafts to transient confinement zones detected by single particle tracking. *Biophys. J*. **82**, 274–284 (2002).
[27] Elson, E. & Magde, D. Fluorescence Correlation Spectroscopy. I. Conceptual Basis and Theory. *Biopolymers* **13**, 1–27 (1974).
[28] Ferko, M. C., Bhatnagar, A., Garcia, M. B., & Butler, P. J. Finite-element stress analysis of a multicomponent model of sheared and focally-adhered endothelial cells. *Annals of Biomedical Engineering* **35** (2), 208–223(2007).
[29] Ferko, M. C., Patterson, B. W., & Butler, P. J. High-resolution solid modeling of biological samples imaged with 3D fluorescence microscopy. *Microsc. Res. Tech*. **69**, 648–655 (2006).
[30] Florian, J. A., et al. Heparan sulfate proteoglycan is a mechanosensor on endothelial cells. *Circ. Res*. **93**, e136–e142 (2003).
[31] Frangos, J. A., Eskin, S. G., McIntire, L. V., & Ives, C. L. Flow effects on prostacyclin production by cultured human endothelial cells. *Science* **227**, 1477–1479 (1985).
[32] Frangos, J. A. & Gudi, S. Shear stress activates reconstituted G-proteins in the absence of protein receptors by modulating lipid bilayer fluidity. *FASEB J*. **11**(3), A521 (1997).
[33] Frangos, J. A., Huang, T. Y., & Clark, C. B. Steady shear and step changes in shear stimulate endothelium via independent mechanisms–superposition of transient and sustained nitric oxide production. *Biochem. Biophys. Res. Commun*. **224**, 660–665 (1996).
[34] Fujiwara, K., Masuda, M., Osawa, M., Kano, Y., & Katoh, K. Is PECAM-1 a mechanoresponsive molecule? *Cell Struct. Funct*. **26**, 11–17 (2001).
[35] Galbraith, C. G., Skalak, R., & Chien, S. Shear stress induces spatial reorganization of the endothelial cell cytoskeleton. *Cell Motil. Cytoskeleton* **40**, 317–330 (1998).
[36] Garcia-Cardena, G., Comander, J. I., Blackman, B. R., Anderson, K. R., & Gimbrone, M. A. Mechanosensitive endothelial gene expression profiles: scripts for the role of hemodynamics in atherogenesis? *Ann. N.Y. Acad. Sci*. **947**, 1–6 (2001).
[37] Garcia-Cardena, G., Oh, P., Liu, J., Schnitzer, J. E., & Sessa, W. C. Targeting of nitric oxide synthase to endothelial cell caveolae via palmitoylation: Implications for nitric oxide signaling. *Proc. Natl. Acad. Sci. U.S.A*. **93**, 6448–6453 (1996).
[38] Gaus, K., Le, L. S., Balasubramanian, N., & Schwartz, M. A. Integrin-mediated adhesion regulates membrane order. *J. Cell Biol*. **174**, 725–734 (2006).
[39] Gautam, M., Shen, Y., Thirkill, T. L., Douglas, G. C., & Barakat, A. I. Flow-activated chloride channels in vascular endothelium: Shear stress sensitivity, desensitization dynamics, and physiological implications. *J. Biol. Chem*. **281** (48), 36492–500 (2006).

[40] Geiger, R. V., Berk, B. C., Alexander, R. W., & Nerem, R. M. Flow-induced calcium transients in single endothelial cells: Spatial and temporal analysis. *Am. J. Physiol*. **262**, C1411–C1417 (1992).
[41] Girard, P. R. & Nerem, R. M. Endothelial cell signaling and cytoskeletal changes in response to shear stress. *Front. Med. Biol. Eng*. **5**, 31–36 (1993).
[42] Girard, P. R. & Nerem, R. M. Shear stress modulates endothelial cell morphology and F-actin organization through the regulation of focal adhesion-associated proteins. *J. Cell Physiol*. **163**, 179–193 (1995).
[43] Gojova, A. & Barakat, A.I. Vascular endothelial wound closure under shear stress: role of membrane fluidity and flow-sensitive ion channels. *J. Appl. Physiol* **98**, 2355–2362 (2005).
[44] Gopalakrishna, P., Chaubey, S. K., Manogaran, P. S., & Pande, G. Modulation of alpha5beta1 integrin functions by the phospholipid and cholesterol contents of cell membranes. *J. Cell Biochem*. **77**, 517–528 (2000).
[45] Goulian, M., et al. Gramicidin channel kinetics under tension. *Biophys. J*. **74**, 328–337 (1998).
[46] Gov, N. S. Diffusion in curved fluid membranes. *Phys. Rev. E. Stat. Nonlin. Soft. Matter Phys*. **73**, 041918 (2006).
[47] Grabowski, E. F., Jaffe, E. A., & Weksler, B. B. Prostacyclin production by cultured endothelial cell monolayers exposed to step increases in shear stress. *Laboratory & Clinical Medicine* **105**, 36–43 (1985).
[48] Green, J. M., et al. Role of cholesterol in formation and function of a signaling complex involving alphavbeta3, integrin-associated protein (CD47), and heterotrimeric G proteins. *J. Cell Biol*. **146**, 673–682 (1999).
[49] Gudi, S., Nolan, J. P., & Frangos, J. A. Modulation of GTPase activity of G proteins by fluid shear stress and phospholipid composition. *Proc. Natl. Acad. Sci. U.S.A*. **95**, 2515–2519 (1998).
[50] Gudi, S. R., Clark, C. B., & Frangos, J. A. Fluid flow rapidly activates G proteins in human endothelial cells. Involvement of G proteins in mechanochemical signal transduction. *Circ. Res*. **79**, 834–839 (1996).
[51] Gullapalli, R. R., Tabouillot, T., Mathura, R., Dangaria, J., & Butler, P. J. Integrated multimodal microscopy, time resolved fluorescence, and optical-trap rheometry: toward single molecule mechanobiology. *J. Biomed. Opt*. **12**(1), 014012 (2007).
[52] Haidekker, M. A., L'Heureux, N., & Frangos, J. A. Fluid shear stress increases membrane fluidity in endothelial cells: A study with DCVJ fluorescence. *Am. J. Physiol Heart Circ. Physiol* **278**, H1401–H1406 (2000).
[53] Hamill, O. P. & Martinac, B. Molecular basis of mechanotransduction in living cells. *Physiol Rev*. **81**, 685–740 (2001).
[54] Helmke, B. P., Goldman, R. D., & Davies, P. F. Rapid displacement of vimentin intermediate filaments in living endothelial cells exposed to flow. *Circ. Res*. **86**, 745–752 (2000).
[55] Honda, H. M., et al. A complex flow pattern of low shear stress and flow reversal promotes monocyte binding to endothelial cells. *Atherosclerosis* **158**, 385–390 (2001).
[56] Ingber, D. E. Mechanobiology and diseases of mechanotransduction. *Ann. Med*. **35**, 564–577 (2003).
[57] Ishida, T., Takahashi, M., Corson, M. A., & Berk, B. C. Fluid shear stress-mediated signal transduction: How do endothelial cells transduce mechanical force into biological responses? *Ann. N.Y. Acad. Sci*. **811**, 12–23 (1997).
[58] Jacobs, E. R., et al. Shear activated channels in cell-attached patches of cultured bovine aortic endothelial cells. *Pflugers Arch*. **431**, 129–131 (1995).

[59] Jacobson, K., Sheets, E. D., & Simson, R. Revisiting the fluid mosaic model of membranes. *Science* **268**, 1441–1442 (1995).
[60] Jalali, S., et al. Integrin-mediated mechanotransduction requires its dynamic interaction with specific extracellular matrix (ECM) ligands. *Proc. Natl. Acad. Sci. U.S.A*. **98**, 1042–1046 (2001).
[61] Jo, H., et al. Differential effect of shear stress on extracellular signal-regulated kinase and N-terminal Jun kinase in endothelial cells. Gi2- and Gbeta/gamma-dependent signaling pathways. *J. Biol. Chem*. **272**, 1395–1401 (1997).
[62] Kaley, G., Koller, A., Messina, E. J., & Wolin, M. S. Role of endothelium-derived vasoactive factors in the control of the microcirculation, in *Cardiovascular Significance of Endothelium-Derived Vasoactive Factors* (ed. Rubanyi, G. M.), 179–195 (Futura Publishing Co., Mount Kisco, NY, 1991).
[63] Kim, D. W., Langille, B. L., Wong, M. K., & Gotlieb, A. I. Patterns of endothelial microfilament distribution in the rabbit aorta in situ. *Circulation Research* **64**, 21–31 (1989).
[64] Koller, A. & Bagi, Z. On the role of mechanosensitive mechanisms eliciting reactive hyperemia. *Am. J. Physiol Heart Circ. Physiol* **283**, H2250–H2259 (2002).
[65] Koller, A., Sun, D., & Kaley, G. Role of shear stress and endothelial prostaglandins in flow- and viscosity-induced dilation of arterioles in vitro. *Circ. Res*. **72**, 1276–1284 (1993).
[66] Korenaga, R., et al. Laminar flow stimulates ATP- and shear stress-dependent nitric oxide production in cultured bovine endothelial cells. *Biochem. Biophys. Res. Commun*. **198**, 213–219 (1994).
[67] Ku, D. N., Giddens, D. P., Zarins, C. K., & Glagov, S. Pulsatile flow and atherosclerosis in the human carotid bifurcation. Positive correlation between plaque location and low oscillating shear stress. *Arteriosclerosis* **5**, 293–302 (1985).
[68] Kuchan, M. J., Jo, H., & Frangos, J. A. Role of G proteins in shear stress-mediated nitric oxide production by endothelial cells. *Am. J. Physiol* **267**, C753–C758 (1994).
[69] Kuo, L., Davis, M. J., & Chilian, W. M. Endothelium-dependent, flow-induced dilation of isolated coronary arterioles. *Am. J. Physiol*. **259**, H1063–H1070 (1990).
[70] Ladbrooke, B. D. & Chapman, D. Thermal analysis of lipids, proteins and biological membranes. A review and summary of some recent studies. *Chem. Phys. Lipids* **3**, 304–356 (1969).
[71] LaDisa, J. F., Jr., et al. Three-dimensional computational fluid dynamics modeling of alterations in coronary wall shear stress produced by stent implantation. *Ann. Biomed. Eng* **31**, 972–980 (2003).
[72] Lakowicz, J. R. *Principles of Fluorescence Spectroscopy* (Springer, Newyork, 1999).
[73] Lange, Y. The rate of transmembrane movement of cholesterol in the human erythrocyte. *J. Biol. Chem*. **256**, 5321–5323 (1981).
[74] Lee, A. G. How lipids affect the activities of integral membrane proteins. *Biochim. Biophys. Acta* **1666**, 62–87 (2004).
[75] Li, S., et al. The role of the dynamics of focal adhesion kinase in the mechanotaxis of endothelial cells. *Proc. Natl. Acad. Sci. U.S.A*. **99**, 3546–3551 (2002).
[76] Li, S., et al. Fluid shear stress activation of focal adhesion kinase. Linking to mitogen-activated protein kinases. *J. Biol. Chem*. **272**, 30455–30462 (1997).
[77] Macdonald, A. G. The homeoviscous theory of adaptation applied to excitable membranes: A critical evaluation. *Biochim. Biophys. Acta Rev. Biomembr*. **1031**, 291–310 (1990).

[78] Magde, D., Elson, E., & Webb, W. W.Fluorescence correlation spectroscopy. II. An experimental realization. *Biopolymers* **13**, 29–61 (1974).
[79] Makino, A., et al. G protein-coupled receptors serve as mechanosensors for fluid shear stress in neutrophils. *Am. J. Physiol Cell Physiol* **290**, C1633–C1639 (2006).
[80] Mateo, C. R. & Douhal, A. A coupled proton-transfer and twisting-motion fluorescence probe for lipid bilayers. *Proc. Natl. Acad. Sci. U.S.A*. **95**, 7245–7250 (1998).
[81] McCormick, S. M., et al. DNA microarray reveals changes in gene expression of shear stressed human umbilical vein endothelial cells. *Proc. Natl. Acad. Sci. U.S.A* **98**, 8955–8960 (2001).
[82] Mitchell, D. C., Lawrence, J. T., & Litman, B. J. Primary alcohols modulate the activation of the G protein-coupled receptor rhodopsin by a lipid-mediated mechanism. *J. Biol. Chem*. **271**, 19033–19036 (1996).
[83] Mochizuki, S., et al. Role of hyaluronic acid glycosaminoglycans in shear-induced endothelium-derived nitric oxide release. *Am. J. Physiol Heart Circ. Physiol* **285**, H722–H726 (2003).
[84] Mouritsen, O. G. & Bloom, M. Mattress model of lipid-protein interactions in membranes. *Biophys*. **46**, 141–153 (1984).
[85] Mouritsen, O. G. & Bloom, M. Models of lipid-protein interactions in membranes. *Ann. Rev. Biophys. & Biomolec. Struct*. **22**, 145–171 (1993).
[86] Muller, J. M., Chilian, W. M., & Davis, M. J. Integrin signaling transduces shear stress–dependent vasodilation of coronary arterioles. *Circulation Research* **80**, 320–326 (1997).
[87] Nagel, T., Resnick, N., Dewey, C. F., Jr., & Gimbrone, M. A., Jr. Vascular endothelial cells respond to spatial gradients in fluid shear stress by enhanced activation of transcription factors. *Arterioscler. Thromb. Vasc. Biol*. **19**, 1825–1834 (1999).
[88] Naruse, K. & Sokabe, M. Involvement of stretch-activated ion channels in Ca2+ mobilization to mechanical stretch in endothelial cells. *Am. J. Physiol* **264**, C1037–C1044 (1993).
[89] Nerem, R. M. Role of mechanics in vascular tissue engineering. *Biorheology* **40**, 281–287 (2003).
[90] Nerem, R. M., Levesque, M. J., & Cornhill, J. F. Vascular endothelial morphology as an indicator of the pattern of blood flow. *J. Biomech. Eng* **103**, 172–176 (1981).
[91] Nielsen, C., Goulian, M., & Andersen, O. S. Energetics of inclusion-induced bilayer deformations. *Biophys. J*. **74**, 1966–1983 (1998).
[92] Oh, P. & Schnitzer, J. E. Segregation of heterotrimeric G proteins in cell surface microdomains. G(q) binds caveolin to concentrate in caveolae, whereas G(i) and G(s) target lipid rafts by default. *Mol. Biol. Cell* **12**, 685–698 (2001).
[93] Ohno, M., Gibbons, G. H., Dzau, V. J., & Cooke, J. P. Shear stress elevates endothelial cGMP. Role of a potassium channel and G protein coupling. *Circulation* **88**, 193–197 (1993).
[94] Olesen, S. P., Clapham, D. E., & Davies, P. F. Haemodynamic shear stress activates a K+ current in vascular endothelial cells. *Nature* **331**, 168–170 (1988).
[95] Packard, B. S. & Wolf, D. E. Fluorescence lifetimes of carbocyanine lipid analogues in phospholipid bilayers. *Biochemistry* **24**, 5176–5181 (1985).
[96] Pries, A. R., Reglin, B., & Secomb, T. W. Structural response of microcirculatory networks to changes in demand: Information transfer by shear stress. *Am. J. Physiol Heart Circ. Physiol* **284**, H2204–H2212 (2003).

[97] Rizzo, V., Sung, A., Oh, P., & Schnitzer, J. E. Rapid mechanotransduction in situ at the luminal cell surface of vascular endothelium and its caveolae. *J. Biol. Chem*. **273**, 26323–26329 (1998).
[98] Saffman, P. G. & Delbruck, M. Brownian motion in biological membranes. *Proceedings of the National Academy of Sciences of the United States of America* **72**, 3111–3113 (1975).
[99] Sato, M., Nagayama, K., Kataoka, N., Sasaki, M., & Hane, K. Local mechanical properties measured by atomic force microscopy for cultured bovine endothelial cells exposed to shear stress. *J. Biomech*. **33**, 127–135 (2000).
[100] Sato, M., Theret, D. P., Wheeler, L. T., Ohshima, N., & Nerem, R. M. Application of the micropipette technique to the measurement of cultured porcine aortic endothelial cell viscoelastic properties. *J. Biomechan. Eng*. **112**, 263–268 (1990).
[101] Satoh, A., Toida, T., Yoshida, K., Kojima, K., & Matsumoto, I. New role of glycosaminoglycans on the plasma membrane proposed by their interaction with phosphatidylcholine. *FEBS Lett*. **477**, 249–252 (2000).
[102] Secomb, T. W., Hsu, R., & Pries, A. R. Effect of the endothelial surface layer on transmission of fluid shear stress to endothelial cells. *Biorheology* **38**, 143–150 (2001).
[103] Secomb, T. W. & Pries, A. R. Information transfer in microvascular networks. *Microcirculation* **9**, 377–387 (2002).
[104] Shinitzky, M. The lipid regulation of receptor functions. *Biomembranes and Receptor Mechanisms* **7**, 135–141 (1987).
[105] Shyy, Y. J., Hsieh, H. J., Usami, S., & Chien, S. Fluid shear stress induces a biphasic response of human monocyte chemotactic protein 1 gene expression in vascular endothelium. *Proc. Natl. Acad. Sci. USA* **91**, 4678–4682 (1994).
[106] Siegel, G., Malmsten, M., & Lindman, B. Flow sensing at the endothelium-blood interface. *Colloids and Surfaces A—Physicochemical and Engineering Aspects* **138**, 345–351 (1998).
[107] Sigurdson, W. J., Sachs, F., & Diamond, S. L. Mechanical perturbation of cultured human endothelial cells causes rapid increases of intracellular calcium. *Am. J. Physiol. Heart Circ. Physiol*. **264**, H1745–H1752 (1993).
[108] Simionescu, M., Simionescu, N., & Palade, G. E. Segmental differentiations of cell junctions in the vascular endothelium: The microvasculature. *J. Cell Biol*. **67**, 863–885 (1975).
[109] Singer, S. J. & Nicolson, G. L. The fluid mosaic model of the structure of cell membranes. *Science* **175**, 720–731 (1972).
[110] Soubias, O., Jolibois, F., Reat, V., & Milon, A. Understanding sterol-membrane interactions, Part II: Complete 1H and 13C assignments by solid-state NMR spectroscopy and determination of the hydrogen-bonding partners of cholesterol in a lipid bilayer. *Chemistry*. **10**, 6005–6014 (2004).
[111] Sowa, G., Pypaert, M., & Sessa, W. C. Distinction between signaling mechanisms in lipid rafts vs. caveolae. *Proc. Natl. Acad. Sci. U.S.A*. **98**, 14072–14077 (2001).
[112] Squire, J. M., et al. Quasi-periodic substructure in the microvessel endothelial glycocalyx: A possible explanation for molecular filtering? *J. Struct. Biol*. **136**, 239–255 (2001).
[113] Stone, P. H., et al. Effect of endothelial shear stress on the progression of coronary artery disease, vascular remodeling, and in-stent restenosis in humans: In vivo 6-month follow-up study. *Circulation* **108**, 438–444 (2003).
[114] Tardy, Y., Resnick, N., Nagel, T., Gimbrone, M. A., Jr., & Dewey, C. F., Jr. Shear stress gradients remodel endothelial monolayers in vitro via a cell

proliferation-migration-loss cycle. *Arterioscler. Thromb. Vasc. Biol*. **17**, 3102–3106 (1997).

[115] Trudell, J. R. Role of membrane fluidity in anesthetic action in, *Drug and Anesthetic Effects on Membrane Structure and Function* (eds. Aloia, R. C., Curtain, C. C., & Gordon, L. M.) 1–14 (Wiley-Liss, Inc., New York, 1991).

[116] Tzima, E., et al. A mechanosensory complex that mediates the endothelial cell response to fluid shear stress. *Nature* **437**, 426–431 (2005).

[117] Wang, Y., et al. Visualizing the mechanical activation of Src 112. *Nature* **434**, 1040–1045 (2005).

[118] Weinbaum, S. & Chien, S. Lipid transport aspects of atherogenesis. *J. Biomech. Eng*. **115**, 602–610 (1993).

[119] Weinbaum, S., Zhang, X., Han, Y., Vink, H., & Cowin, S. C. Mechanotransduction and flow across the endothelial glycocalyx. *Proc. Natl. Acad. Sci. U.S.A*. **100**, 7988–7995 (2003).

[120] Wentzel, J. J., et al. Shear stress, vascular remodeling and neointimal formation. *J. Biomech*. **36**, 681–688 (2003).

[121] Wolf, A. A., Fujinaga, Y., & Lencer, W. I. Uncoupling of the cholera toxin-G(M1) ganglioside receptor complex from endocytosis, retrograde Golgi trafficking, and downstream signal transduction by depletion of membrane cholesterol. *J. Biol. Chem*. **277**, 16249–16256 (2002).

[122] Zaidel-Bar, R., Kam, Z., & Geiger, B. Polarized downregulation of the paxillin-p130CAS-Rac1 pathway induced by shear flow. *J. Cell Sci*. **118**, 3997–4007 (2005).